Spectroelectrochemical Studies of Olefins. 3.[1] The Dimerization Mechanism of the 4,4'-Dimethoxystilbene Cation Radical in the Absence and Presence of Methanol[2]

Eberhard Steckhan

Contribution from the Organisch-Chemisches Institut der Universität Münster, D-4400 Münster, Orléans-Ring 23, West Germany. Received September 28, 1977
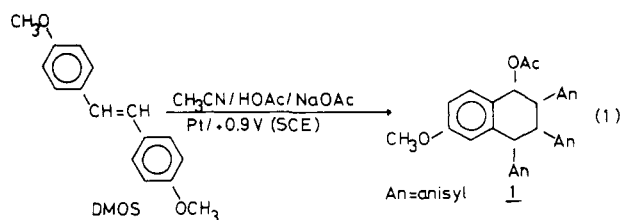
Abstract: By systematic elucidation of the mechanisms of the synthetically valuable anodic oxidation of olefins insight may be gained for optimization of the electrosyntheses and prediction of the reaction paths of unknown olefins. As an excellent example for studying the kinetics and mechanisms of anodic olefin oxidations 4,4'-dimethoxystilbene (DMOS) has been examined. The electrochemically generated DMOS cation radical dimerizes to give high yields of a tetralin derivative (electrolyte: acetonitrile/acetic acid/acetate), 2,3,4,5-tetraanisyltetrahydrofuran (solvent: acetonitrile), or 1,2,3,4-tetraanisyl-1,4-dimethoxybutane (solvent: acetonitrile/methanol or dichloromethane/methanol). The kinetics of the reactions have been determined by two transmission spectroelectrochemical methods, single potential step chronoabsorptometry and open circuit relaxation, observing the time-dependent absorbance change of $DMOS^{+}\cdot$ at 425 and 530 nm. The reaction in the absence of a nucleophile was found to obey the rate law $d[DMOS^{+}\cdot]/dt = -2k_{12}[DMOS^{+}\cdot]^2 - 2k_5[DMOS^{+}\cdot][DMOS]$ with the rate constant for the radical dimerization $k_{12} = 5k_5$. For the reaction in the presence of methanol the rate law was evaluated to be $d[DMOS^{+}\cdot]/dt = -2k_{12}[DMOS^{+}\cdot]^2 - k_{19}[DMOS^{+}\cdot][CH_3OH]$ with $k_{19} = \frac{1}{2}k_{12}$. Values of 1.45×10^4 to 2.85×10^4 s^{-1} M^{-1} have been calculated for k_{12} under different conditions. The conclusion can be drawn that in the absence of a nucleophile, the radical dimerization of $DMOS^{+}\cdot$ dominates over its electrophilic attack to the parent olefin while in the presence of excess methanol the reaction of $DMOS^{+}\cdot$ with the nucleophile predominates.

Introduction

The anodic oxidation of olefins leads to the formation of a wide spectrum of products of great preparative interest, and in particular, dimers.[3-8] Better knowledge of the reaction mechanism is necessary if the attempt to optimize a synthesis or to predict a certain reaction path will be successful. The study of the kinetics of the reactive intermediates is the most important way to the elucidation of a reaction mechanism. The primary intermediate in the anodic oxidation of olefins is the cation radical. Generation of the cation radical at optically transparent electrodes (OTE) allows either its UV–visible spectrum to be obtained by the use of a rapid scanning spectrometer[1b] or the study of the kinetics by analyzing the time-dependent absorbance change at its absorbance maximum.[1a,9-11]

The anodic dimerization of olefins can either take place by radical dimerization or by electrophilic attack of the cation radical to the parent compound. Preparative scale electrolysis under controlled potential has demonstrated that both pathways seem to be followed dependent on the kind of olefins.[5,12] But mechanistic data are too limited to allow a prediction of the reaction pathway. Therefore a systematic study of the kinetics and mechanisms of anodic olefin oxidations is under way.

4,4'-Dimethoxystilbene (DMOS) is of special interest as its cation radical is of moderate reactivity thereby facilitating the kinetic study but still undergoes dimerization in the presence of acetate ion (eq 1) in a clean reaction.[13] The results of con-

trolled potential electrolysis, cyclic voltammetry, and a kinetic and mechanistic study of the anodic DMOS oxidation in the absence and presence of a nucleophile based on the spectroelectrochemical technique are reported.

Technique of Kinetic Measurement

The kinetic study of the electrochemical dimerization of DMOS in acetonitrile/methanol at the potential of the first anodic wave is based on two different transmission spectroelectrochemical methods: spectroscopic observation of the $DMOS^{+}\cdot$ concentration change at 425 and 530 nm during a chronoamperometric experiment (single potential step chronoabsorptometry) and during a subsequent open circuit relaxation period (OCR).[9-11,14] In both cases experimentally determined normalized absorbances (A_N) are compared with digitally simulated dimensionless working curves applying the computer simulation method of Feldberg.[15] The absorbance from the single potential step experiment (A_k) is normalized to the absorbance value in the absence of a chemical follow-up reaction ($A_{k=0}$). $A_{k=0}$ is determined by extrapolation of the linear part of the A vs. $t^{1/2}$ plot at short times. In the case of the open circuit relaxation experiment the absorbance at any time t^* after disconnection of the electrode (A_t^*) is normalized to the absorbance value at the moment the cell is disconnected (A_{oc}). The concentration profiles of the chemical components at the start of the OCR experiment have to be exactly reproduced by the simulated concentration profiles. This is achieved by setting the fluxes of DMOS and $DMOS^{+}\cdot$ equal to zero at the electrode surface when the simulated A_N value reaches the experimental A_N value at the time the circuit is opened (t_{oc}). To get a reasonable signal to noise ratio of the optical signal, signal averaging had to be applied.

For single potential step experiments rate constants can also be determined from the time t_{max} at which the absorbance maximum occurs.[16]

Results

Voltammetric Study. The cyclic voltammograms of DMOS in acetonitrile/0.2 M $LiClO_4$ in the absence and presence of methanol are shown in Figure 1. In the absence of methanol two anodic peaks at +0.92 and +1.14 V vs. SCE are observed. If high scan rates and iR compensation are applied, a reduction peak at +0.86 V vs. SCE appears on the reverse scan. In the presence of methanol a third anodic peak at +1.29 V is observed. When the direction of the voltage sweep is reversed
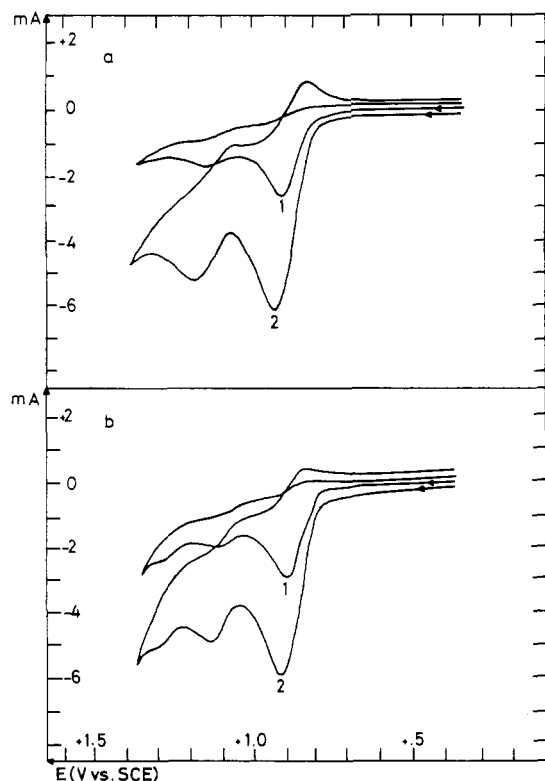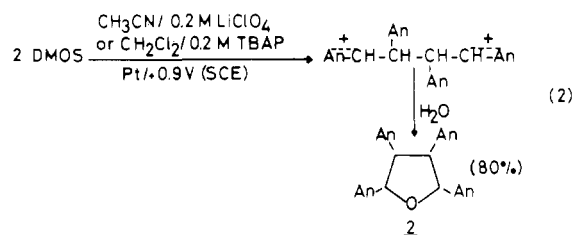
Figure 1. Cyclic voltammograms of DMOS at sweep rates of 1.8 (1) and 7.2 V/s (2): (a) DMOS (2 mM) in $CH_3CN/LiClO_4$ (0.2 M); (b) DMOS (2 mM), CH_3OH (10 mM) in $CH_3CN/LiClO_4$ (0.2 M).

after the first anodic peak at +0.92 V the corresponding reduction peak at +0.86 V is observed, if scan rates of at least 320 mV/s are used (Figure 2). The first anodic wave corresponds to the exchange of one electron per molecule as shown by comparison with the peak current of ferrocene under corresponding conditions. The electrochemically reversible redox couple with peak potentials of +0.92 and +0.86 V, respectively,

is due to the formation and reduction of the DMOS cation radical. The second oxidation wave at +1.14 V is due to the generation of the DMOS dication ($DMOS^{2+}$). The smaller peak current as compared with the first anodic wave indicates that $DMOS^+\cdot$ undergoes further chemical reaction.[13] This conclusion is supported by the observation that the peak current ratio of the second and first anodic waves as well as the peak current ratio of the first anodic and cathodic waves are approaching one with increasing scan rate. The peak current of the first anodic peak does not change by addition of different amounts of methanol while the corresponding reduction peak, however, is lowered.

Product Study. The anodic oxidation of DMOS at a platinum anode at the controlled potential of the first anodic wave using acetonitrile/0.2 M $LiClO_4$ as electrolyte after aqueous workup results in the formation of almost exclusively 2,3,4,5-tetraanisyltetrahydrofuran (**2**) (eq 2). The corre-

$$2 \text{ DMOS} \xrightarrow[\text{Pt}/+0.9V \text{ (SCE)}]{\substack{CH_3CN/ \ 0.2 \text{ M } LiClO_4 \\ \text{or } CH_2Cl_2/0.2 \text{ M } TBAP}} \overset{+}{An}\text{-CH-CH-CH-CH}\overset{+}{=}\text{An}$$

(2)

sponding compound is formed during anodic oxidation of styrene in aqueous acetonitrile.[17] Only very small amounts of 4,4'-dimethoxybenzophenone can be detected as a side product. Exactly 1.0 faraday/mol is consumed.

Under corresponding conditions using solvent mixtures of acetonitrile/25% methanol or dichloromethane/25% methanol the main product is the dimethoxylated open-chain dimer 1,2,3,4-tetraanisyl-1,4-dimethoxybutane (**3**) in 75% current yield (eq 3). As side products the three dimethoxylated monomers **4**, **5**, and **6** are formed in 10% current yield all together. Compound **6** has undergone an aryl group migration. Exactly 1.0 faraday/mol is consumed until total turnover of DMOS is achieved.
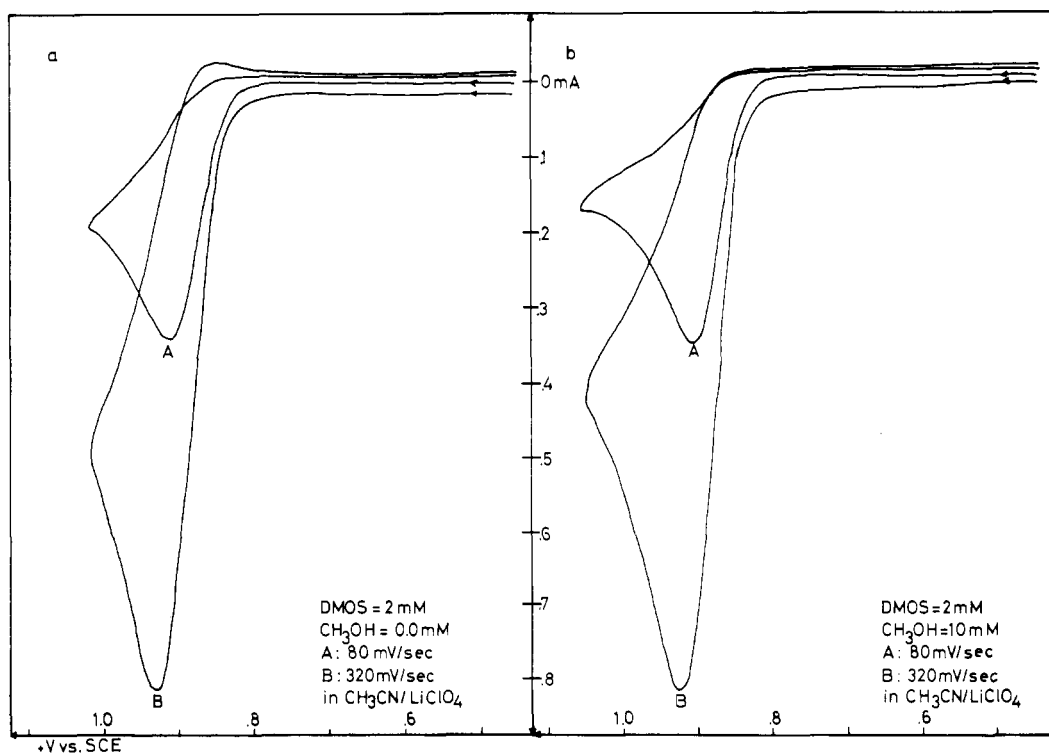

Figure 2. Cyclic voltammograms of DMOS reversing the sweep direction after the first anodic peak.
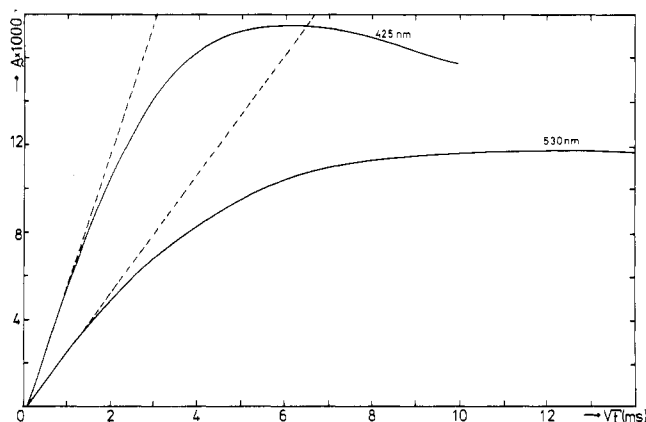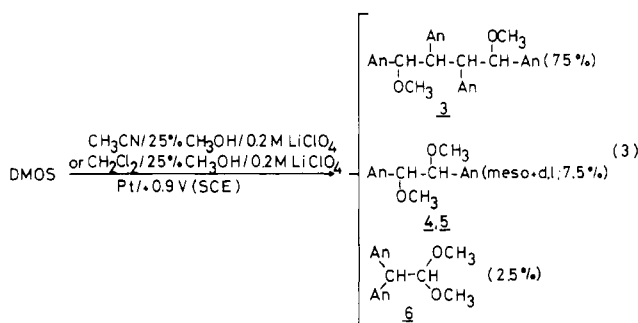
Figure 3. $A/t^{1/2}$ behavior of the 425- and 530-nm absorbance maxima of DMOS$^+$.

Spectroscopic Study. The UV–visible spectra of intermediates formed during a potential step experiment at an OTE under diffusion controlled conditions have been acquired using a rapid scanning spectrometer with signal averaging under computer control.[1b] Two absorption bands at 425 and 530 nm have been observed. By comparison with known spectra of similar compounds the 530-nm band was assigned to the DMOS$^+$.

Analysis of the time-dependent absorbance change at both wavelengths (425, 530 nm) supplies additional information about the nature of the absorbing species. At short times the absorbance at these wavelengths increased linearly with the square root of the time if the potential pulse was slightly more positive than the potential of the first anodic peak (Figure 3). This is an indication that both absorbance bands belong to the primary reaction intermediate, the DMOS cation radical.[16] However, at 530 nm the absorbance maximum occurs at longer times $t_{\max}$ as compared with the 425-nm band, giving rise to suspicion that an absorbance band of a product or a stable intermediate is overlapping with the 530-nm band of DMOS$^+$.[16] As the product does not absorb at this wavelength, a likely compound could be the protonated form of DMOS. This was checked by dissolving DMOS in CH$_2$Cl$_2$/trifluoroacetic acid/trifluoroacetic anhydride (1:1:1). The purple solution shows an absorbance band at 536 nm but no ESR signal. As during the course of the reaction, protons are generated, and partial protonation of DMOS can be expected. The DMOS cation radical can be excluded as the absorbing species because no ESR signal is obtained.

Kinetic Study of the Anodic DMOS Dimerization in Acetonitrile/LiClO$_4$. The dimerization of DMOS$^+$ to form the cyclized dimeric product **2** can principally either take place by electrophilic attack of DMOS$^+$ on the parent olefin or by radical dimerization. For both pathways many mechanistic variations are possible. For all of them dimensionless working curves have to be digitally simulated for the electrochemical experiment and have to be compared with curves from experimental data which have been obtained by optically monitoring

the DMOS$^+$ concentration at 425 and 530 nm. Comparison of calculated and experimentally determined values for the most important mechanistic possibilities are shown in Figures 4 and 5.

No agreement of data can be obtained for a first-order reaction in [DMOS$^+$] and [DMOS], as expected when electrophilic attack of DMOS$^+$ on DMOS is assumed. Scheme I shows the corresponding reaction sequence.

Scheme I
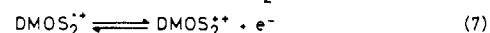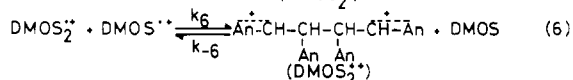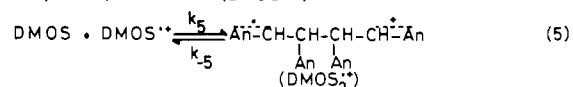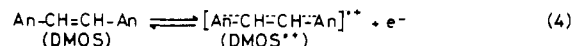
If the electrophilic attack of DMOS$^+$ on DMOS (eq 5) is irreversible ($k_5 \gg k_{-5}$) and rate determining, and if electron transfer from DMOS$_2$$^+$ takes place predominantly by heterogeneous reaction (eq 7) ($k_6 \leq 0.1k_5$), the rate law for this so-called "ECE mechanism"[1a,14] is given by

$$d[\text{DMOS}^+\cdot]/dt = -k_5[\text{DMOS}][\text{DMOS}^+\cdot] \quad (9)$$

If the homogeneous electron transfer from DMOS$_2$$^+$ (eq 6) dominates over the heterogeneous one ($k_6 \geq 100k_5$), the rate law for this "half-regeneration mechanism"[1a,14] is obtained (eq 10), assuming steady-state conditions for the concentration of DMOS$_2$$^+$.

$$d[\text{DMOS}^+\cdot]/dt = -2k_5[\text{DMOS}][\text{DMOS}^+\cdot] \quad (10)$$

For both mechanisms the slopes of the working curves are too steep (see curves with short dashes in Figures 4 and 5). If rate constants are calculated on the basis of these mechanisms, decreasing values are obtained with increasing time for both experiments.

Assuming a fast equilibrium between (DMOS + DMOS$^+$) and DMOS$_2$$^+$ (eq 5) with the homogeneous electron transfer (eq 6) as rate-determining step, the rate law is second order in [DMOS$^+$] and first order in [DMOS]:

$$d[\text{DMOS}^+\cdot]/dt = -2k_6K_5[\text{DMOS}^+\cdot]^2[\text{DMOS}] \quad (11)$$

If the calculation of the rate constant is based on this mechanism, increasing values are obtained with increasing time (dash-point curves in Figures 4 and 5).

For a slow equilibrium (eq 5) explicit values for the rate constants have to be inserted into the computer program for digitally simulating the working curves. If a value of 50 is assumed for k_5/k_{-5}, the experimental data points for the single potential step experiment follow the working curve quite well. But for the OCR experiment the digitally determined A_N values at longer times drop very slowly while the experimental data are fast approaching zero (dotted lines in Figures 4 and 5).

If a radical dimerization (Scheme II) of DMOS$^+$ is as-

Scheme II
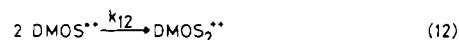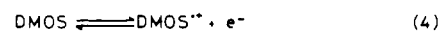
sumed, the rate law for [DMOS$^+$] is given by eq 13.

$$d[\text{DMOS}^+\cdot]/dt = -2k_{12}[\text{DMOS}^+\cdot]^2 \quad (13)$$
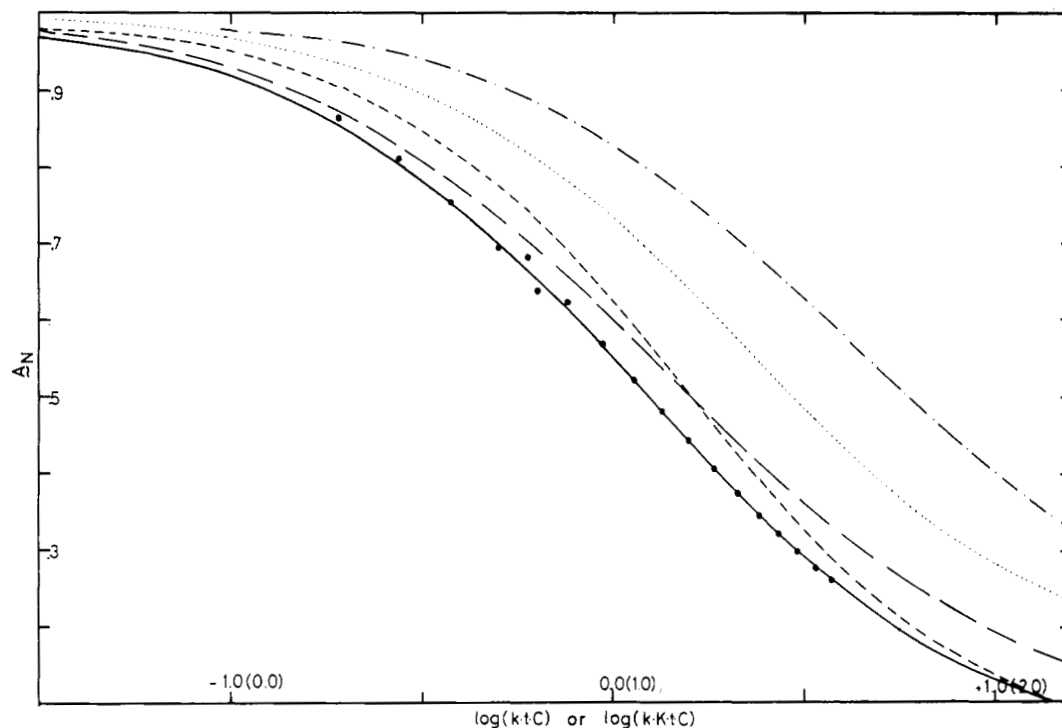
Figure 4. Digitally simulated spectroelectrochemical working curves for single potential step chronoabsorptometry observing $DMOS^+\cdot$ in the absence of a nucleophile: assuming rate law 10 (small dashed line); assuming rate law 11 (dash-point line); assuming a slow equilibrium (eq 5) with k_5/k_{-5} = 50 (dotted line); assuming rate law 13 (long dashed line); assuming rate law 14 (solid line), and comparison of the working curves with experimentally determined values (observation of $DMOS^+\cdot$ at 425 nm) assuming a mechanism based on rate law 14 (●).
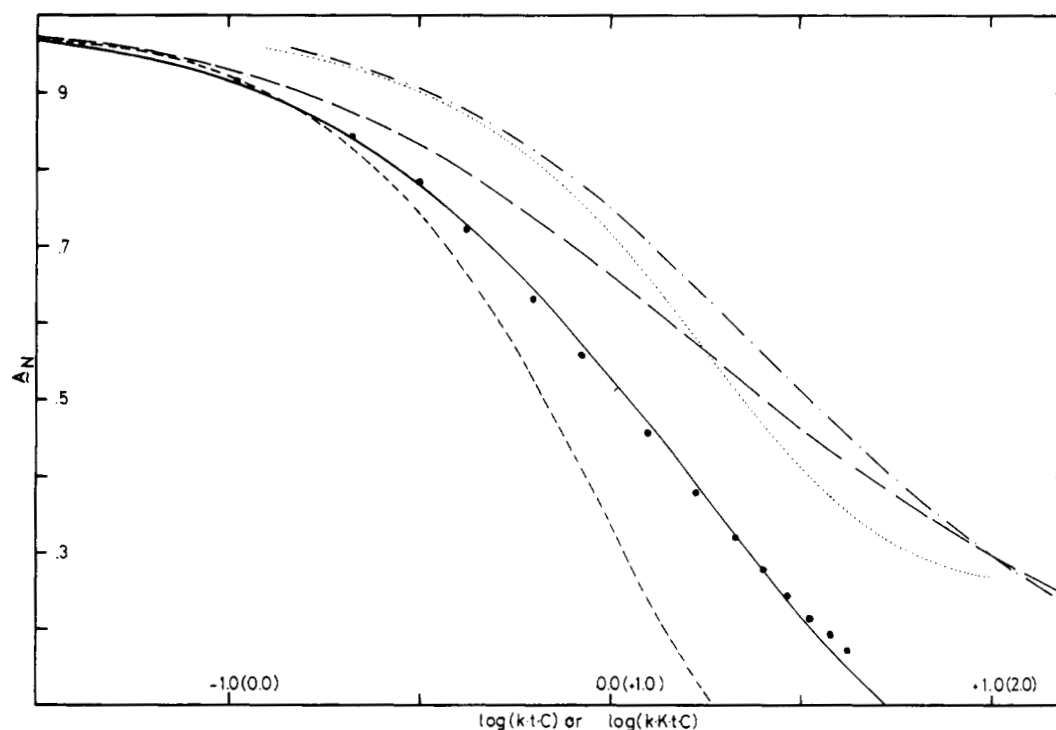
Figure 5. Digitally simulated spectroelectrochemical working curves for open circuit relaxation observing $DMOS^+\cdot$ in the absence of a nucleophile: assuming rate law 10 (small dashed line); assuming rate law 11 (dash-point line); assuming a slow equilibrium (eq 5) with k_5/k_{-5} = 50 (dotted line); assuming rate law 13 (long dashed line); assuming rate law 14 (solid line), and comparison of the working curves with experimentally determined values (observation of $DMOS^+\cdot$ at 424 nm) assuming a mechanism based on rate law 14 (●).

As compared with the experimental data the simulated working curves for the radical dimerization mechanism are too flat. But the deviation for the single potential step experiment is much smaller than for the OCR experiment (curves with long dashes in Figures 4 and 5) giving rise to the suspicion that parallel reactions may take place, one being second order in $[DMOS^+\cdot]$ and the other being first order in $[DMOS^+\cdot]$. Indeed experimental and simulated data are consistent for the rate law

$$d[DMOS^+\cdot]/dt = -2k_{12}[DMOS^+\cdot]^2 - 2k_5[DMOS][DMOS^+\cdot] \quad (14)$$

Table I. Experimentally Determined Rate Constants for Radical Dimerization of DMOS$^+$· $(k_{12})^a$ in Acetonitrile/LiClO$_4$. Observation of DMOS$^+$· at 425 nm^b

Single potential step chronoabsorptometry			Open circuit relaxation	
$k_{12} \times 10^{-4},^c$ s^{-1} M^{-1}	$k_{12} \times 10^{-4},^d$ s^{-1} M^{-1}	LiClO$_4$, M	$k_{12} \times 10^{-4},^e$ s^{-1} M^{-1}	LiClO$_4$, M
1.71	1.80	0.2	2.10	0.2
1.48	1.69	0.2	1.45	0.2
1.65	1.77	0.2	1.73	0.2
1.45		0.1		
1.75		0.3		

^{a} Rate constant k_5 for electrophilic attack of DMOS$^+$· on DMOS: $k_5 = \frac{1}{5}k_{12}$. ^{b} DMOS = 2 mM in CH$_3$CN/LiClO$_4$; 20 °C. ^{c} Averages of at least 14 data points between 4 and 100 ms. ^{d} Determined from time t_{max} of absorbance maximum. ^{e} Averages of at least 12 data points between 2.5 and 100 ms.

with k_5 being $\frac{1}{5}k_{12}$. The rate constants calculated on the basis of this rate law (eq 14) show no significant deviation with time and are in accordance for both experimental methods, single potential step and OCR (solid lines in Figures 4 and 5). They are summarized in Table I. A salt effect is not observed.

Measurements of the disappearance of DMOS$^+$· at 530 nm as compared with 425 nm gave similar results. But because of overlapping bands at 530 nm the agreement of experimental data points with the simulated curves was not as good.

Kinetic Study of the Anodic Dimerization of DMOS in the Presence of Methanol. The kinetic study in the presence of methanol has been performed under true second-order conditions. The concentration ratios of DMOS and CH$_3$OH were 1:1, 1:2, and 1:5. Experiments under second-order conditions give much more evidence than those under pseudo-first-order conditions (excess methanol).[18] The results of the single potential step and OCR experiments during observation of [DMOS$^+$·] at 425 nm immediately show that the rate of disappearance of DMOS$^+$· is increasing with increasing methanol concentration (Figures 6 and 7). Therefore all mechanisms can be ruled out in which [CH$_3$OH] is not incorporated in the rate law.

Also no agreement of experimental and calculated data can be obtained, if the rate law for the disappearance of DMOS$^+$· is second order in [DMOS$^+$·] and first or second order in [CH$_3$OH].

The regeneration mechanism (Scheme III) can also be ruled

Scheme III

$$\text{DMOS} \rightleftharpoons \text{DMOS}^{+\cdot} + \text{e}^- \quad (4)$$

$$\text{DMOS} + \text{DMOS}^{+\cdot} \underset{k_{-5}}{\overset{k_5}{\rightleftharpoons}} \text{DMOS}_2^{+\cdot} \quad (5)$$

$$\text{DMOS}_2^{+\cdot} + \text{CH}_3\text{OH} \underset{k_{-15}}{\overset{k_{15}}{\rightleftharpoons}} \underset{\underset{\text{OCH}_3}{|}}{\text{An-CH-CH-CH-CH-An}} + \text{H}^+ \quad (15)$$
$$(\text{DMOS}_2\text{M}^\cdot)$$

$$\text{DMOS}_2\text{M}^\cdot + \text{DMOS}^{+\cdot} \underset{k_{-16}}{\overset{k_{16}}{\rightleftharpoons}} \underset{\underset{\text{OCH}_3}{|}}{\text{An-CH-CH-CH-CH-An}} + \text{DMOS} \quad (16)$$
$$(\text{DMOS}_2\text{M}^+)$$

$$\text{DMOS}_2\text{M}^+ + \text{CH}_3\text{OH} \longrightarrow \text{Product} \quad (17)$$

out because the simulated working curves (dotted lines in Figures 6 and 7) are too flat as compared with experimental data. The reaction rate is mainly influenced by equilibrium 5 and barely by the methanol concentration.

Irreversible reaction of DMOS$^+$· with methanol and subsequent dimerization (Scheme IV) follows rate law 18.

$$d[\text{DMOS}^+\cdot]/dt = -k_{19}[\text{DMOS}^+\cdot][\text{CH}_3\text{OH}] \quad (18)$$

This mechanism (Scheme IV) comes closest to the observed

Table II. Experimentally Determined Rate Constants for Radical Dimerization of DMOS$^+$· (k_{12}) and Irreversible Reaction of DMOS$^+$· with CH$_3$OH (k_{19}) in Acetonitrile/0.2 M LiClO$_4$ in the Presence of Methanol. Observation of DMOS$^+$· at 425 nm^a

Single potential step chronoabsorptometry $k_{12} \times 10^{-4}$, s^{-1} M^{-1} ^{b} [DMOS]:[CH$_3$OH]			Open circuit relaxation $k_{12} \times 10^{-4}$, s^{-1} M^{-1} ^{c} [DMOS]:[CH$_3$OH]		
1:1	1:2	1:5	1:1	1:2	1:5
2.73	3.44	2.26	2.45	2.85	2.10
(2.52)	(2.14)	(2.14)			
2.72	2.44	2.22	2.73	2.83	2.26
(2.52)	(2.14)	(2.14)			
$k_{19} \times 10^{-4}$, s^{-1} M^{-1}			$k_{19} \times 10^{-4}$, s^{-1} M^{-1}		
1.36	1.22	1.13	1.22	1.42	1.05
(1.26)	(1.07)	(1.07)			
1.36	1.22	1.11	1.36	1.41	1.13
(1.26)	(1.07)	(1.07)			

^{a} DMOS = 2 mM in CH$_3$CN/LiClO$_4$ 0.2 M; 20 °C. ^{b} Averages of at least 11 data points between 4 and 50 ms. Values in parentheses determined from t_{max} of absorbance maximum. ^{c} Averages of at least 11 data points between 2.5 and 50 ms (1:1), 2.5 and 40 ms (1:2), 1.25 and 25 ms (1:5).

Scheme IV

$$\text{DMOS} \rightleftharpoons \text{DMOS}^{+\cdot} + \text{e}^- \quad (4)$$

$$\text{DMOS}^{+\cdot} + \text{CH}_3\text{OH} \xrightarrow{k_{19}} \underset{\underset{\text{HOCH}_3}{|}}{\text{An-CH-CH-An}} (\text{DMOSM}^{+\cdot}) \quad (19)$$

$$2 \text{ DMOSM}^{+\cdot} \longrightarrow \text{Product} \quad (20)$$

reaction (dashed lines in Figures 6 and 7), but the dependence of the reaction rate on the methanol concentration is higher than observed.

With small methanol concentrations, one must expect that, parallel to the reaction with methanol, reaction of DMOS$^+$· partially takes place by radical dimerization, the reaction path observed in the absence of a nucleophile. Indeed, experimental and simulated data are in agreement for parallel reactions of radical dimerization (Scheme II) and irreversible reaction of DMOS$^+$· with methanol (Scheme IV) assuming $k_{19} = \frac{1}{2}k_{12}$ (solid lines in Figures 6 and 7). Rate law 21 has been used for digital simulations.

$$d[\text{DMOS}^+\cdot]/dt = -2k_{12}[\text{DMOS}^+\cdot]^2$$
$$- k_{19}[\text{DMOS}^+\cdot][\text{CH}_3\text{OH}] \quad (21)$$

The rate constants, calculated on the basis of rate law 21, show no significant time-dependent deviation and are independent of methanol concentration. They are in accordance with both experimental methods employed, and in addition to this the value of k_{12} in the presence of methanol is very close to that obtained for the experiments in the absence of a nucleophile. Experimental values for k_{12} and k_{19} are summarized in Table II.

Observation of DMOS$^+$· at 530 nm gave similar results but some time-dependent deviations of the rate constants due to overlapping spectral bands of DMOS$^+$· and the protonated DMOS at this wavelength occurred.

Discussion

The electrochemical oxidation of DMOS at the potential of the first anodic wave is an uncomplicated one-electron reaction as indicated by controlled potential coulometry giving 1.0 faraday/mol. The dimeric products **2** (in acetonitrile after aqueous workup) and **3** (in acetonitrile/25% methanol) can be isolated in high yields.

Cyclic voltammetry indicates that the olefin radical cation is the primary intermediate. Because the peak current of the

Figure 6. Digitally simulated spectroelectrochemical working curves for single potential step chronoabsorptometry observing DMOS$^+$· in the presence of methanol (DMOS/methanol concentration ratio 1:1, 1:2, 1:5): assuming a regeneration mechanism (Scheme III) (dotted lines); assuming rate law 18 (dashed lines); assuming rate law 21 (solid lines), and comparison of the working curves with experimentally 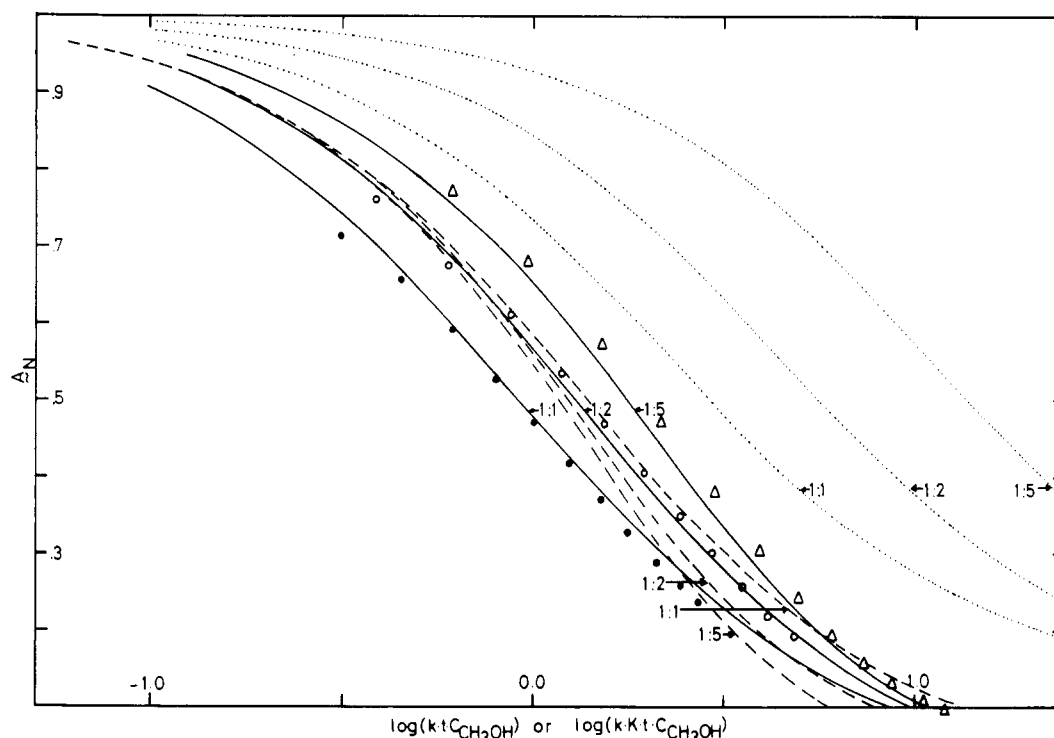determined values (observation of DMOS$^+$· at 425 nm) assuming a mechanism based on rate law 21 ($\bullet$ = 1:1, $\circ$ = 1:2, $\triangle$ = 1:5).
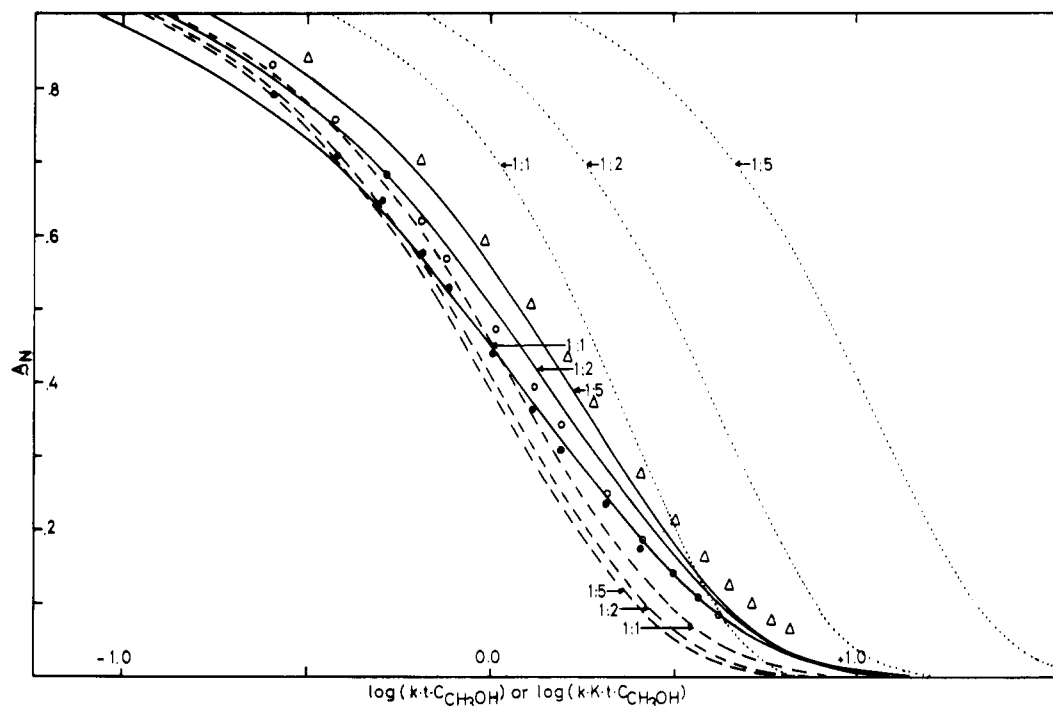
Figure 7. Digitally simulated spectroelectrochemical working curves for open circuit relaxation observing DMOS$^+$· in the presence of methanol (DMOS/methanol concentration ratio 1:1, 1:2, 1:5): assuming a regeneration mechanism (Scheme III) (dotted lines); assuming rate law 18 (dashed lines); assuming rate law 21 (solid lines), and comparison of the working curves with experimentally determined values (observation of DMOS$^+$· at 425 nm) assuming a mechanism based on rate law 21 ($\bullet$ = 1:1, $\circ$ = 1:2, $\triangle$ = 1:5).

first anodic wave is not increased by addition of methanol, it can be concluded that the radical cation intermediate formed by reaction of DMOS$^+$· with methanol is more difficult to oxidize than the parent olefin. The additional oxidation wave observed in the presence of methanol at +1.29 V could be attached to this intermediate. In addition the cyclic voltammo-

gram in acetonitrile indicates an electrochemically reversible anodic oxidation of DMOS ($E_{pa} - E_{pc}$ = 60 mV at slow sweep rates) and a chemical follow-up reaction, which is accelerated by addition of methanol. The observation of the reduction peak of DMOS$^+$· at vert high sweep rates and iR compensation is indicating a moderate reactivity of DMOS$^+$·.

The occurrence of the absorbance maximum with λ_{max} 530 nm at a three times higher t_{max} as compared with the 425-nm band can be explained in three different ways: products are absorbing at 530 nm; stable intermediates are absorbing at this wavelength; two different compounds in equilibrium with each other are absorbing at 425 and 530 nm, respectively. As the isolated products do not absorb at 530 nm, they can be ruled out as an explanation for the differences in t_{max}. If an equilibrium of DMOS$^+$· and a complex like (DMOS$^+$····DMOS) is assumed, the t_{max} for both absorbance maxima should be almost identical for a fast equilibrium. For a slow equilibrium, however, the absorbance of the complex at short times should not increase linearly with $t^{1/2}$ but with a certain time delay,[19] as shown by digital simulation. The most probable explanation for the higher t_{max} at 530 nm is overlapping of the band with that of the protonated form of DMOS which absorbs at 536 nm as shown by protonation with trifluoroacetic acid in dichloromethane. Therefore, the most reliable results of the kinetic measurement by spectroelectrochemistry can be obtained at 425 nm.

Kinetics and mechanisms of the anodic dimerization of DMOS have been studied in acetonitrile and acetonitrile/methanol, respectively, by two different spectroelectrochemical methods. In the presence of methanol three different concentration ratios of DMOS and CH$_3$OH have been applied. All together eight different experiments, practically independent of each other, have been performed. Only if the results of all eight experiments can be brought into agreement can the underlying mechanism be expected to describe the reaction adequately. This agreement could only be obtained if parallel reactions are assumed to take place in both media.

In the absence of a nucleophile, radical dimerization (Scheme II) takes place simultaneously with the electrophilic attack of DMOS$^+$· on DMOS (Scheme I) according to the "half-regeneration mechanism". The mean value of the rate constant of the radical dimerization has been evaluated to be $k_{12} = 1.69 \times 10^4$ s^{-1} M^{-1} with a standard deviation of 0.2×10^4. The rate constant of the electrophilic attack of DMOS$^+$· on DMOS was calculated to be $k_5 = 0.34 \times 10^4$ s^{-1} M^{-1} with a standard deviation of 0.04×10^4. Participation of the regeneration mechanism in the overall reaction is much smaller during the single potential step experiment than during the OCR experiment. The reason is the high concentration of DMOS$^+$· in a thin reaction layer at the electrode surface during its diffusion-controlled generation thereby favoring its radical dimerization. After opening the circuit and stopping the DMOS$^+$· generation, attack of DMOS$^+$· on DMOS becomes more important with increasing time and decreasing DMOS$^+$· concentration. During preparative electrolysis of DMOS in acetonitrile under diffusion-controlled conditions the radical dimerization mechanism should by far be the dominating reaction.

There might be one more reasonable mechanistic possibility for anodic dimerization of DMOS in acetonitrile: that is, the radical dimerization of DMOS$^+$· paralleled by irreversible reaction of DMOS$^+$· with residual water which might be present in small amounts despite all precautions. But if experimental data are brought into agreement with this mechanism for the single potential step experiment, the rate constants calculated for the OCR experiment show a time-dependent increase. The reason is that the water concentration in the single potential step experiment influences the reaction rate more than the concentration of DMOS which is being consumed at the electrode surface. However, minor participation of the reaction of the DMOS cation radical with water cannot totally be excluded.

In the presence of methanol, irreversible reaction of DMOS$^+$· with methanol and subsequent dimerization (Scheme IV) takes place simultaneously with the radical di-

merization of DMOS$^+$· (Scheme II). With only small concentrations of methanol present it is obvious that besides the reaction with the nucleophile, the reaction which is favored in the absence of a nucleophile will also take place. The mean value of the rate constant evaluated for the radical dimerization of DMOS$^+$· is calculated to be $k_{12} = 2.42 \times 10^4$ s^{-1} M^{-1} with a standard deviation of 0.26×10^4. This value agrees reasonably well with the one obtained in acetonitrile without a nucleophile present thereby further supporting the assumed reaction mechanism. The slightly higher value may be a medium effect. The value for the rate constant of the reaction of DMOS$^+$· with methanol is half of k_{12} ($k_{19} = 1.21 \times 10^4$ s^{-1} M^{-1}). During preparative electrolysis of DMOS in acetonitrile/25% methanol the reaction of DMOS$^+$· with methanol is clearly favored. With the high methanol concentrations present the radical dimerization of DMOS$^+$· cannot compete with reaction 19.

Experimental Section

Infrared spectra were recorded on a Perkin-Elmer 157 spectrophotometer. ^{1}H NMR spectra were obtained with a Varian HA-100 spectrometer using tetramethylsilane as an internal standard. ^{13}C NMR spectra were determined by means of a Bruker Physik AG spectrometer WH 90 with CDCl$_3$ as solvent. Chemical shifts were measured relative to the solvent and converted to the Me$_4$Si scale by using the factor 77.0. Ultraviolet spectra were recorded on a Leitz Unicam SP 800 A spectrophotometer. Mass spectra were obtained with a MAT 111 GLC/MS combination or a MAT SM 1 spectrometer. Yields, calculated with respect to electrochemical charge consumed, are determined by quantitative GLC using a Varian 1440 chromatograph in connection with a Kipp & Zonen BD 8 recorder, an Autolab Minigrator as integrator, and a glass column, 1.7 m, ϕ 2 mm, 4% SE-30, Chromosorb W, AWD CMS, 100/120 mesh. Microanalyses were performed by Mikroanalytisches Laboratorium Beller, Göttingen, Germany.

Acetonitrile and dichloromethane (Merck) were spectroquality, dried by passing them through a column of neutral alumina (Merck), and stored over neutral alumina. Reagent grade DMOS (Aldrich) was purified by recrystallization from alcohol.

Cyclic voltammetry was performed in the spectroelectrochemical cell which has been described.[1b] A Wenking Potential Control Amplifier PCA 72 L together with iR compensation by a positive feedback circuit[20] was used. Voltage functions were produced by a Wavetek 133 LF waveform generator. A Hewlett-Packard 7045 A X-Y recorder was used.

Preparative electrolysis was performed using a Wenking Potential Control Amplifier PCA 72 L together with an electronic integrator.[21]

Anodic Oxidation of DMOS in Acetonitrile. DMOS (1.2 g, 5.0 mmol) in CH$_3$CN (100 mL) containing LiClO$_4$ (0.2 M) was subjected to anodic oxidation at a platinum electrode (7 cm^2) at a controlled potential of +0.67 V vs. Ag/AgNO$_3$ (0.1 M) and a current of 10 mA in an undivided cell under N$_2$ atmosphere. DMOS was only partially soluble in the solvent but went into solution during the course of the reaction. After consumption of 486 A s (5 mF) the current dropped to 1 mA and the electrolysis was stopped. The solution was hydrolyzed with 50 mL of H$_2$O and extracted several times with dichloromethane and ether. The organic phase was washed with small amounts of water and dried over MgSO$_4$, and the solvent was evaporated. The residue (1.8 g) was analyzed by GLC (4% SE-30) and GLC/MS coupling. Small amounts of 4,4'-dimethoxybenzophenone (<4%) could be identified by comparison with an authentic sample. **2** consisted of several isomers as indicated by GLC/MS. **2** was purified by precipitation as an amorphous powder from alcohol. Because of the composition from several isomers no clean melting point could be obtained. Current yield of **2** (quantitative GLC, 4% SE-30) 80%. **2**: IR (KBr pellet) 1608, 1580, 1500, 1460, 1442, 1302, 1250, 1176, 1110, 1033, 830 cm^{-1}; UV (CH$_3$CN) λ_{max} (log ϵ) 276 (3.9), 284 nm (sh); mass spectrum (70 eV) m/e (rel intensity) 495 (4), 478 (8), 360 (100), 329 (28), 252 (36), 240 (30), 227 (96), 135 (60), 121 (30); ^{1}H NMR (CCl$_4$, Me$_4$Si) δ 3.61 (s, 6 H), 3.67 (s, 6 H), 3.63 (2 H), 6.3–7.3 (m, 18 H). The ^{1}H NMR signal at δ 3.63 is hidden by the singlet for the methoxy groups at δ 3.61 and 3.67 but can be observed, if the methoxy protons are shifted by Eu(fod)$_3$. The protons at C$_2$ and C$_5$ must be

covered by the signals of the aromatic protons. The extreme low-field shift of the signals might be due to a special sterical arrangement of the four highly hindered aromatic rings. A ^{13}C NMR signal at δ 87.1 (CDCl$_3$) for C$_2$ and C$_5$ is supporting the structure.

Anal. (C$_{32}$H$_{32}$O$_5$) C, H.

Anodic Oxidation of DMOS in Acetonitrile/Methanol. DMOS (1.2 g, 5.0 mmol) in CH$_3$CN/CH$_3$OH (3:1, 100 mL) containing LiClO$_4$ (0.2 M) was subjected to anodic oxidation at a platinum electrode (7 cm^2) at a controlled potential of +0.67 V vs. Ag/AgNO$_3$ (0.1 M) and a current of 10 mA in an undivided cell under N$_2$ atmosphere. DMOS was only partially soluble in the solvent but went into solution during the course of the reaction. After consumption of 490 A s (5 mF) the current dropped to 1 mA and the electrolysis was stopped. The solvent was removed under vacuum, and the residue was dissolved in small amounts of dichloromethane and three times washed with 30 mL of H$_2$O to remove LiClO$_4$. The organic phase was dried (MgSO$_4$) and the solvent evaporated. The residue (1.5 g) was analyzed by GLC/MS coupling. Current yields (quantitative GLC, 4% SE-30) follow: **3** (75%), **4 + 5** (7.5%), **6** (2.5%). Compound **3** was isolated from the crude product by preparative TLC (petroleum ether/ether, 2:1) and purified by recrystallization from CCl$_4$ and subsequent sublimation. **3**: mp 234-237 °C; IR (KBr pellet) 1608, 1502, 1460, 1304, 1242, 1174, 1092, 1034, 882, 830, 814, 786 cm^{-1}; ^{1}H NMR (CCl$_4$, Me$_4$Si) δ 2.84 (s, 6 H), 3.28 (s, 2 H), 3.63 (s, 6 H), 3.74 (s, 6 H), 3.84 (s, 2 H), 6.4-6.8 (s + m, 16 H); ^{13}C NMR (CDCl$_3$) δ 55.0, 55.4, 56.7 83.0, 112.7, 127.7, 131.4, 131.7, 133.5, 158.0; mass spectrum (70 eV) m/e (rel intensity) 542 (0.3), 479 (0.3), 478 (0.6), 359 (2.0), 346 (1.0), 271 (4), 240 (10), 227 (10), 225 (9), 152 (43), 151 (100), 136 (10), 135 (22), 121 (8), 108 (5), 91 (3), 75 (4).

Anal. (C$_{34}$H$_{38}$O$_6$) C, H.

Compounds **4, 5,** and **6** could not be isolated because of the small yields. They were identified by mass spectra (70 eV): **4** m/e (rel intensity) 270 (8), 255 (5), 227 (9), 151 (100), 135 (22), 75 (13); **5** m/e (rel intensity) 270 (12), 255 (5), 227 (12), 151 (100), 135 (17), 75 (20); **6** m/e (rel intensity) 270 (60), 255 (25), 227 (60), 135 (12), 119 (17), 113 (12), 75 (100).

Kinetic Study. The instrumentation has previously been described[1a] but instead of a Ag/AgCl reference electrode a pseudoreference silver wire was inserted into the solution next to the working electrode to minimize uncompensated resistance effects. The optical signal was subjected to signal averaging by a Princeton Applied Research TDH 9 Waveform Eductor to optimize the signal to noise ratio. The electronic circuit to disconnect the working electrode in the OCR experiment has been described elsewhere.[22] The solvents were dried over alumina and solvents and solutions were transferred to the volumetric flasks and the spectroelectrochemical cell by use of gas-tight syringes. Solutions not containing methanol were stored over neutral alumina.

References and Notes

(1) For other parts in the series, see (a) E. Steckhan, *Electrochim. Acta,* **22,** 395–399 (1977); (b) E. Steckhan and D. A. Yates, *Ber. Bunsenges. Phys. Chem.,* **81,** 369–374 (1977).
(2) Financial support by Deutsche Forschungsgemeinschaft und Fonds der Chemischen Industrie is gratefully acknowledged.
(3) H. Schäfer and E. Steckhan, *Angew. Chem.,* **81,** 532 (1969).
(4) D. Koch, H. Schäfer, and E. Steckhan, *Chem. Ber.,* **107,** 3640–3657 (1974).
(5) R. Engels, H. Schäfer, and E. Steckhan, *Justus Liebigs Ann. Chem.,* 204–224 (1977).
(6) H. Baltes, E. Steckhan, and H. Schäfer, *Chem. Ber.,* submitted for publication.
(7) F. Beck, "Elektroorganische Chemie", Verlag Chemie, Weinheim/Bergstr., Germany, 1974, pp 241–243.
(8) N. L. Weinberg, "Techniques of Chemistry", Vol. V, Part I, A. Weissberger, Ed., Wiley, New York, N.Y., 1974, pp 355–410.
(9) T. Kuwana and N. Winograd, *Electroanal. Chem.,* **7,** 1–78 (1974).
(10) T. Kuwana, *Ber. Bunsenges. Phys. Chem.,* **77,** 858–871 (1973).
(11) T. Kuwana and W. R. Heineman, *Acc. Chem. Res.,* **9,** 241–248 (1976).
(12) D. Koch, Thesis, Göttingen, 1973, pp 69–71.
(13) (a) V. D. Parker and L. Eberson, *Chem. Commun.,* 340 (1969); (b) L. Eberson and V. D. Parker, *Acta Chem. Scand.,* **24,** 3553–3562 (1970).
(14) R. F. Broman, W. R. Heineman, and T. Kuwana, *Faraday Discuss. Chem. Soc.,* **56,** 16–27 (1973).
(15) S. W. Feldberg, *Electroanal. Chem.,* **3,** 199–296 (1969).
(16) G. C. Grant and T. Kuwana, *J. Electroanal. Chem. Interfac. Electrochem.,* **24,** 11–21 (1970).
(17) E. Steckhan and H. Schäfer, *Angew. Chem.,* **86,** 480–481 (1974).
(18) H. N. Blount, *J. Electroanal. Chem. Interfac. Electrochem.,* **42,** 271–274 (1973).
(19) N. R. Armstrong, R. K. Quinn, and N. E. Vanderborgh, *J. Phys. Chem.,* **81,** 657 (1977).
(20) E. R. Borwn, D. E. Smith, and G. L. Booman, *Anal. Chem.,* **40,** 1411–1423 (1968).
(21) Electronic integrator is based on a current to voltage converter (Teledyne/Philbrick 4709) and a MOS counter (Intersil ICM 7208). Design by H. Luftmann.
(22) H. N. Blount, N. Winograd, and T. Kuwana, *J. Phys. Chem.,* **74,** 3231–3236 (1970).

Formation of Dithioether Dications in the Anchimerically Assisted Reduction of Monosulfoxides of Mesocyclic and Acyclic Dithioethers

Joyce Takahashi Doi* and W. Kenneth Musker

Department of Chemistry, University of California, Davis, California 95616. Received October 10, 1977

Abstract: The reduction of the mesocyclic sulfoxide, 1,5-dithiacyclooctane 1-oxide (**1**) by iodide in aqueous acid proceeds ~10^6 times more rapidly than simple sulfoxides. The rate is essentially independent of iodide and shows a second-order dependence on acid concentration. The accelerated rate of reduction is attributed to an anchimeric assistance by the transannular thioether group which leads to an intermediate dithioether dication, **3**. This same dithioether dication has been isolated previously in the oxidation of 1,5-dithiacyclooctane (**2**) in nonaqueous solvents. 2,6-Dithiaheptane 2-oxide (**6**) is the acyclic analogue of **1**. The rate of reduction with HI is also zero order in iodide, suggesting that neighboring-group participation also occurs in an acyclic compound to give a five-membered-ring dithioether dication (**7**). In contrast to **1** and **6**, 1,4-dithiane 1-oxide behaves like a simple sulfoxide. Thus, the rapid formation of dithioether dications in the reactions of **1** and **6** suggests that these species should be considered as possible intermediates in reactions where a positive charge is induced on a sulfur atom in the proximity of a thioether group.

A transannular interaction in the mesocyclic dithioether, 1,5-dithiacyclooctane (**2**) has been suggested to explain its mass spectrum,[1] its electrochemistry,[2] and its facile oxidation to the dithioether dication (**3**) in nonaqueous solvents.[3] Mechanistic studies on the HI reduction of monosulfoxides[4-9] have indicated that reaction proceeds through a protonated